Shaping of Airplane Fuselages for Minimum Drag

S.S. Dodbele* and C.P. van Dam†
Vigyan Research Associates Inc., Hampton, Virginia
P.M.H.W. Vijgen‡
University of Kansas, Lawrence, Kansas
and
B.J. Holmes§
NASA Langley Research Center, Hampton, Virginia

Recent technological advances in airplane construction techniques and the use of materials employing bonded and milled aluminum skins and composite materials allow aerodynamic surfaces to be produced without significant waviness and roughness. These construction advances have resulted in excellent opportunities for reducing airplane drag by increasing the extent of natural laminar flow. In this paper, the feasibility of extensive regions of laminar flow on airplane fuselages is discussed. Pressure distribution, boundary-layer development, transition location, and drag coefficient are calculated for a number of body shapes, including a representative business aircraft fuselage. Extensive runs of natural laminar flow are predicted for regions of favorable pressure gradient under smooth surface conditions. The adequacy of existing transition prediction methods applied to bodies is also discussed. A woeful lack of experimental data at representative length Reynolds numbers is noted. A computational design procedure has been developed to generate low-drag body shapes, and results are presented.

Nomenclature

C_D = drag coefficient
C_P = pressure coefficient
f_r = fineness ratio, body length/maximum diameter
H = boundary-layer shape factor, $=\delta^*/\theta$
K_1 = curvature at X_m
k_1 = nondimensional curvature at $X_m = -2x_m f_r K_1 L$
L = body length
M = Mach number
n = logarithmic exponent of T-S wave growth ratio
R_i = profile radius at X_i
R_L = Reynolds number based on freestream conditions and body length
R_n = radius of curvature at the nose
R_s = Reynolds number based on local conditions and surface length
R_V = Reynolds number based on freestream conditions and $V^{1/3}$
R_x = Reynolds number based on local conditions and axial length
R_θ = Reynolds number based on local conditions and θ
r_i = nondimensional profile radius at X_i, $=2f_r R_i/L$
r_n = nondimensional radius of curvature at the nose, $=4x_m f_r R_n/L$
s = surface length starting at nose
s_i = nondimensional profile slope at X_i, $=-2f_r(x_i-x_m)S_i/(L-r_i)$
V = body volume
v = local velocity
U_∞ = freestream velocity
X = axial coordinate, starting at nose of body
X_i = axial location of inflection point
X_m = axial location of maximum diameter
x = nondimensional axial location, $=X/L$
x_i = nondimensional location of inflection point, $=X_i/L$
x_m = nondimensional axial location of maximum diameter, $=X_m/L$
x_{tr} = nondimensional axial length coordinate at transition
z = nondimensional body ordinate
δ^* = boundary-layer displacement thickness
θ = boundary-layer momentum thickness
ϕ = semitrailing-edge angle at the tail of the body

Introduction

IN recent years, airplane construction material and fabrication methods have improved greatly, resulting in the production of airframe surfaces that accurately match the design shape. Recent flight tests[1,2] have demonstrated that extensive runs of laminar boundary-layer flow can be obtained over regions of favorable pressure gradient on modern production airplane surfaces and provide a significant reduction in profile drag. A major portion of the past research effort for achieving and maintaining natural laminar flow (NLF) has been focused on aircraft wings. Fuselage shaping to increase the extent of NLF has received much less attention in the literature except for sailplane bodies and hydrodynamic bodies.

The importance of fuselage drag reduction is indicated by an example in Fig. 1, in which profile-drag buildup is shown for a typical transport jet.[3] The fuselage generates about 50% of total profile drag for the all-turbulent airplane. However, it is estimated that the contribution of the turbulent fuselage to airplane profile drag increases to more than 70% if extensive regions of laminar flow are achieved on the wing and the tail surfaces. Another example, which depicts the influence of boundary-layer transition location on body drag coefficient, is presented in Table 1. In Table 1, drag coefficients for an axisymmetric body of fineness ratio 6.14 are listed for various transition locations. It is inferred from the table that the delay of laminar to turbulent transition by about 27% of the body length ($x_{tr} = 0.050$ to 0.322)

Presented as Paper 86-0316 at the AIAA 24th Aerospace Sciences Meeting, Reno, NV, Jan. 6-9, 1986; received April 24, 1986; revision received Nov. 24, 1986.

*Research Scientist. Senior Member AIAA.
†Research Scientist, presently Assistant Professor, Department of Mechanical Engineering, University of California, Davis. Member AIAA.
‡Doctoral Candidate. Student Member AIAA.
§Head, Flight Applications Branch. Member AIAA.

reduces body drag coefficient by as much as 30%. References 4 and 5 also highlight the benefits of achieving laminar flow on various airframe components.

The present study investigates the design of fuselage shapes that can result in extensive regions of laminar flow for commuter, business, and transport airplanes at cruise conditions. The adequacy of existing transition prediction methods applied to bodies is discussed. A computational design procedure has been developed to obtain fuselage geometries for considerable extent of laminar flow and, hence, for low drag.

Previous Research

Althaus[6] demonstrated that reduction in airplane drag can be achieved through shape modifications of sailplane fuselages at low length Reynolds numbers ($R_L = 7.1 \times 10^6$). Radespiel[7] reported improved performance for a glider configuration through wing repositioning and fuselage "waisting." Hertel[8] was one of the first researchers to draw attention to the suitability of certain streamline shapes for achieving natural laminar boundary-layer flow on fuselages of transport aircraft. Carmichael[9] was the first to conduct an innovative experimental study in a low-turbulence environment on a body at high length Reynolds numbers. In the Pacific Ocean, a body of fineness ratio 3.33 developed by revolving the coordinates of a NACA 6-series airfoil was tested. The characteristics of this unpowered tail-boomed body were measured over a Reynolds number range of $20\text{–}40 \times 10^6$ (based on body length) and transition-length Reynolds numbers of $14\text{–}18 \times 10^6$ were obtained. Boundary-layer transition from laminar to turbulent flow apparently occurred beyond the point of maximum thickness. These results indicate that a low fineness ratio and a proper shape can produce a strong favorable pressure gradient (and therefore a strong flow acceleration) on the forebody of the configuration. Consequently, the boundary layer stays laminar over an appreciable distance. Boltz et al.[10] conducted an investigation in the Ames 12-ft low-turbulence pressure tunnel to determine the boundary-layer transition characteristics of two bodies of revolution (fineness ratios 7.5 and 9.0) at subsonic speeds with $R_L \simeq 10^7$. It was concluded that for a given Mach number the pressure distribution was a primary factor in determining the level of transition Reynolds number, and small increases in the favorable pressure gradients over the forward portion of the body resulted in significant increases in the transition Reynolds number. Meier and Kreplin[11] conducted detailed boundary-layer measurements over a range of incidence angles at a maximum length Reynolds number of about 10^7 on a prolate spheriod of fineness ratio 6.

Computational drag minimization studies have been conducted by Dalton and Zedan,[12] Parsons et al.,[13,14] Pinebrook and Dalton,[15,16] and Wolfe and Oberkampf.[17] Barger[18] investigated the effect of forebody shaping to achieve natural laminar flow on cruise missiles flying at high subsonic Mach numbers. Since length Reynolds numbers, Mach numbers, or body fineness ratios used in these studies are not representative of general-aviation, business, and transport airplanes, results from these studies are of limited application in the present work. Also, some of the preceding studies used axial source distributions to represent the various body shapes. Use of surface singularities (surface panel methods) instead of axial singularities eliminates some of the problems recently described by Hess[19] (also see Ref. 20).

A low-order surface panel code (VSAERO) developed by Maskew[21] has been used to represent the body in the present

All-turbulent surfaces		Laminar lifting surfaces	
Nacelles and misc	5.2%	Nacelles and misc	7.6%
Fuselage	48.7%	Fuselage	70.2%
Empennage	14.3%	Empennage	6.9%
Wing	31.8%	Wing	15.3%
Nacelle and others	.0010	Nacelle and others	.0010
Fuselage	.0092	Fuselage	.0092
Empennage	.0027	Empennage	.0009
Wing	.0060	Wing	.0020
Total profile C_D	.0189	Total profile C_D	.0131

Fig. 1 Profile drag buildup for all-turbulent transport jet and airplane with laminar lifting surfaces (Ref. 3).

Table 1 Drag coefficients for axisymmetric body (Fig. 10)

x (Transition location)	C_D[a]
0.322	0.0260
0.15	0.0343
0.10	0.0362
0.05	0.0374

[a]Reference area for C_D calculation was frontal area.

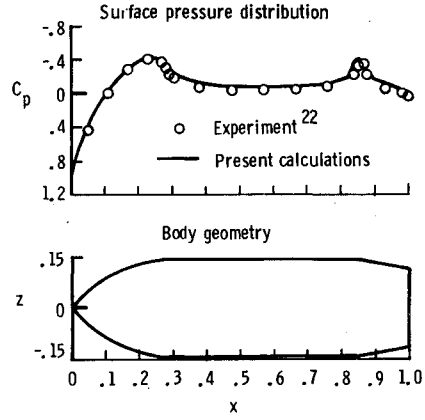

Fig. 2 Surface pressure distribution and geometry for a body tested (see Ref. 22) at $M = 0.404$ and $\alpha = 0.06$ deg.

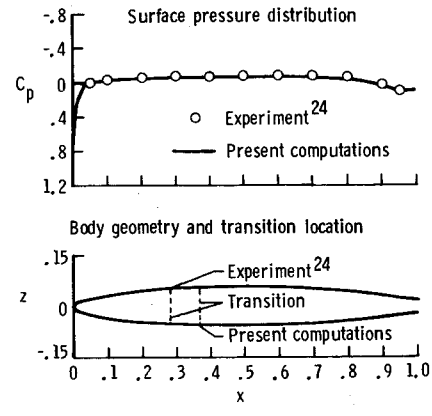

Fig. 3 Pressure distribution, geometry, and transition location for $f_r = 9$ ellipsoid at $\alpha = 0$ deg, $R_L = 13.98 \times 10^6$.

study. The method is based on piecewise constant doublet and source singularities and can take into account the effects of compressibility.

Surface Pressure and Boundary-Layer Calculations

To validate the surface panel method,[21] inviscid pressure distributions have been obtained for several configurations. The effect of the viscous boundary layer adjacent to the body is calculated by integral boundary-layer methods. The laminar part of the boundary layer is calculated by Thwaites' method with Curle's modifications. Boundary-layer transition is predicted by Granville's procedure. Nash and Hick's method is used for the turbulent boundary-layer calculations. Laminar separation/turbulent reattachment calculations are performed empirically using Gaster's measurements.

Very good agreement between measured and calculated surface pressure coefficients was obtained for a body of revolution tested by Fox in the NASA Langley high-speed 7- × 10-ft wind tunnel.[22] In Fig. 2, the results are shown for the configuration, an axisymmetric body composed of an ogival nose, a cylindrical center body, and a truncated conical afterbody. Surface pressure data are plotted as function of the orifice location for orifices on the longitudinal meridian. Pressure coefficients obtained by using the surface singularity method are also presented in Fig. 2.

Groth[23] reports measurements of pressure and boundary-layer transition in wind tunnels and measurement of boundary-layer transition in flight on an ellipsoid of revolution. Figure 3 presents the surface pressure distribution and transition location for the ellipsoid of revolution of fineness ratio 9. The viscous calculations were conducted for $R_L = 13.98 \times 10^6$. Although the pressure distributions compare well, the predicted transition location does not agree very well with the experimental data. The calculated transition-length Reynolds number was 5.08×10^6. Granville's boundary-layer transition criterion, which is used in the present computation, predicts transition further downstream than actually happened in the experiment. (In private communication, Dr. W. Pfenninger has indicated that the F94 boundary-layer transition data appear to be adversely affected by excessive engine sound levels.) The same discrepancy is noticed when the length Reynolds number is increased to 22.03×10^6. Kaups[24] also computed transition location for this ellipsoid by using Granville's criterion, and he too found that at these two Reynolds numbers, transition is predicted at points further downstream than was observed in the experiments (in flight and wind tunnel). Kaups concluded that none of the transition-prediction methods, including the e^9 method of Smith and Gamberoni, gave consistently satisfactory answers for the ellipsoid. These results illustrate that for bodies with flat pressure distributions at low Mach numbers where Tollmien-Schlichting instability may grow rapidly, a considerable amount of uncertainty exists in the calculation of transition location. Transition prediction for such pressure distributions will be particularly difficult because of sensitivity to disturbances in the test environment.

Next, a low-drag body of revolution of fineness ratio 4.5 with a long favorable pressure gradient forebody is considered. Hansen and Hoyt[25] measured the drag and boundary-layer intermittency experimentally and calculated the pressure distribution. In Fig. 4, a comparison is shown between Hansen and Hoyt's data and the present computational results. In the present study, transition is predicted at the point of laminar separation ($x = 0.67$) for $R_L = 10.86 \times 10^6$. This result agrees well with the theoretically predicted transition location $x = 0.68$, at laminar separation, reported by Hansen and Hoyt.

Another low-drag body (called X-35) was studied by Parsons et al.[14] and is analyzed here. The calculated velocity distribution agrees very well with that presented in Ref. 14, as shown in Fig. 5. Parsons et al. used the Michel-e^9 correlation[26] to predict boundary-layer transition. The results plotted in Fig. 6 indicate that Michel-e^9 criterion was not met for the X-35 body, and transition at laminar separation was predicted at $x = 0.68$ for $R_L = 37.14 \times 10^6$. For the identical conditions, Granville's transition criterion is more conservative with transition predicted at $x = 0.35$. The discrepancy in the results obtained by using Michel and Granville transition criteria as applied to bodies has been analyzed further by applying the H-R_x transition criterion by Wazzan et al.[27] The H-R_x method (for bodies R_X is replaced by R_s) correlates the boundary-layer shape factor $H = \delta^*/\theta$ and R_s at transition. The results plotted in Fig. 7 show transition to occur at $x = 0.25$. (Although the H-R_x method predicted a transition location that agreed very well with the experimental results for a 13:1 Reichardt's body,[27] the accuracy of the method for bodies with low to moderate fineness ratio is not known yet.)

The empirical transition prediction methods were also analyzed by performing a linear stability analysis of the laminar boundary layer using the SALLY code,[28] whereas input to this program is provided by a modified version of the HARRIS finite-difference boundary-layer code.[29] In Fig. 8, the logarithmic disturbance amplitude ratio or "n factor" is plotted as a function of the nondimensional axial distance for a range of Tollmien-Schlichting disturbance frequencies. These curves indicate the growth of an initially infinitesimal disturbance of a given frequency in the laminar boundary layer. The envelope of the curves in Fig. 8 shows that an n factor of 9 is reached at $x = 0.185$; at $x = 0.25$, the location at

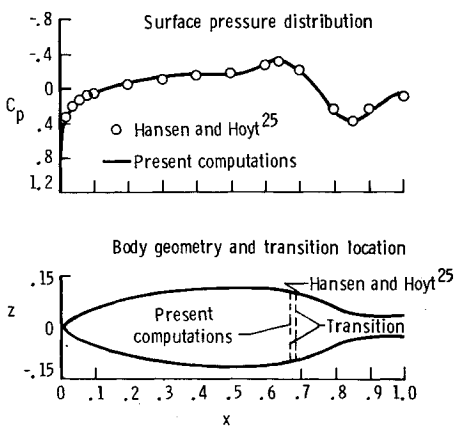

Fig. 4 Pressure distribution, geometry, and transition location for $f_r = 4.5$ body of revolution at $\alpha = 0$ deg and $R_L = 13.41 \times 10^6$.

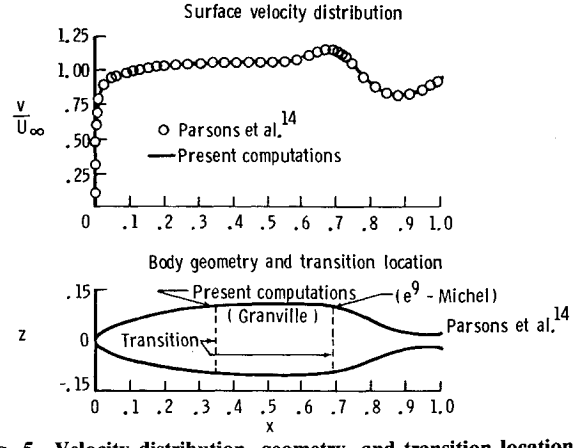

Fig. 5 Velocity distribution, geometry, and transition location for X-35 body at $\alpha = 0$ deg and $R_L = 37.14 \times 10^6$.

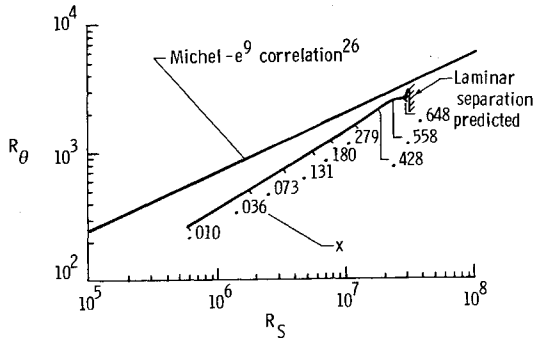

Fig. 6 Boundary-layer development and transition location for X-35 using Michel-e^9 correlation ($\alpha=0$ deg, $R_L=37.14\times10^6$).

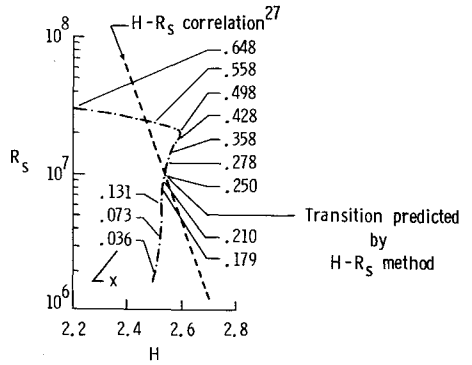

Fig. 7 Boundary-layer development and transition location for X-35 using H-R_x method ($\alpha=0$ deg, $R_L=37.14\times10^6$).

which transition was predicted by H-R_x method, the n factor is about 12.5. (Natural transition in low-disturbance wind tunnels generally corresponds to a maximum "n" of 9–11. Maximum "n" up to 15 have been observed in flight.) Unfortunately, there are no experimental results available on the X-35 body to check the predictions provided by the various methods.

Next, a representative business aircraft fuselage of fineness ratio 6.14 was analyzed. Inviscid pressure distributions on the upper and lower surface were calculated and are presented in Fig. 9. Transition location was predicted using Granville's criterion at a unit Reynolds number of 1×10^6/ft ($R_L=40.86\times10^6$) and is noted on the figure (transition Reynolds number range of $4.1\text{–}16.0\times10^6$). It is not possible to analyze these kinds of practical nonaxisymmetric bodies by using axial singularity distributions. Furthermore, the Granville transition prediction assumes no three-dimensional boundary-layer instability effects. While this assumption could affect the validity of the transition prediction, the value of that limitation (say in terms of Reynolds number) is not known.

Finally a body of revolution whose maximum diameter and length correspond to those of the previous configuration was considered. This configuration can also be thought of as a special case of the previously analyzed body obtained by setting the longitudinal camber equal to zero. Inviscid pressure distributions and transition locations are presented in Fig. 10 for $\alpha=0$ deg.

The pressure distributions for the bodies considered herein agreed very well with results from other sources, although the transition predictions did not agree well with the available experimental results. This disagreement between theory and experiment is due in part to the fact that the bodies considered here have very flat pressure gradients. In addition, the transition criteria are based on two-dimensional correlations and they are used in higher ranges of length Reynolds number than originally intended. Most of the correlations are based on experiments conducted at relatively low length Reynolds numbers. Experimental results them-

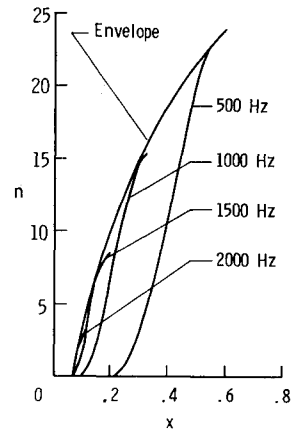

Fig. 8 Logarithmic amplification of Tollmien-Schlichting disturbance frequencies for X-35 ($\alpha=0$ deg, $R_L=37.14\times10^6$).

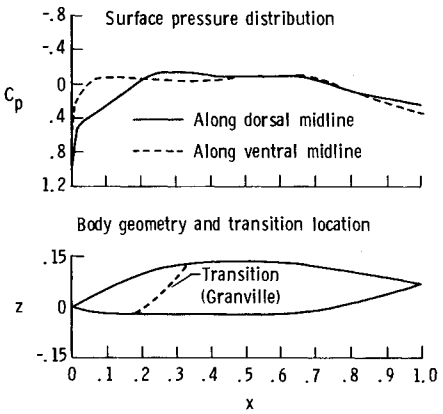

Fig. 9 Pressure distribution, geometry, and transition location for a representative business aircraft fuselage ($\alpha=0$ deg, $R_L=40.86\times10^6$).

Table 2 Convergence of the design variables ($f_r=6.14$, $R_L=40.86\times10^6$, $\alpha=0$ deg)

No. of iterations	x_m	k_1	r_n	r_i	s_i	x_i	ϕ	x_{tr}	C_D[a]
Initial	0.55550	0.17109	0.35000	0.40000	2.2867	0.85531	10.011	0.360	0.0247
1	0.55000	0.17109	0.35000	0.47144	1.7324	0.85000	10.905	0.359	0.0237
2	0.55000	0.17109	0.35000	0.46918	1.6660	0.85260	10.976	0.359	0.0237
3	0.55491	0.17109	0.35000	0.46956	1.6660	0.85609	10.980	0.365	0.0236
4	0.55292	0.17109	0.35000	0.46949	1.6660	0.85604	10.984	0.365	0.0236
5	0.55162	0.17109	0.35000	0.46969	1.6660	0.85596	10.986	0.364	0.0235
6	0.55151	0.17109	0.35000	0.46971	1.6660	0.85595	10.986	0.359	0.0238
7	0.55145	0.17109	0.34987	0.46974	1.6660	0.85598	10.987	0.364	0.0235
8	0.55145	0.17109	0.34986	0.46974	1.6660	0.85596	10.987	0.364	0.0235

[a]Reference area for C_D calculation was frontal area.

selves could also be influenced by turbulence levels and acoustic disturbances.

In summary, the state of the art in transition prediction on bodies of $f_r = 4$–10 (of interest for aircraft fuselages) is very poor. To provide useful methods for transition prediction in flight, methods must be developed to include the effects of compressibility, nonparallel boundary-layer flow, surface curvature, Tollmien-Schlichting wave stretching, and cross-flow vorticity in the laminar boundary layer. Detailed boundary-layer transition experiments at high length Reynolds numbers are necessary to improve understanding of transition phenomena over fuselages.

Drag Estimation on Axisymmetric Bodies

Drag coefficient C_D is computed from the momentum deficit in the wake of the body using Young's formula.[30] The turbulent boundary layer grows much faster than the laminar boundary layer and creates most of the wake momentum deficit. In the present investigation, the drag coefficient is defined as being the maximum drag coefficient computed as a function of axial location x on the axisymmetric body using Young's formula.[30] In Fig. 11, drag values obtained with the present method are compared with measured drag data[25] for the previously discussed body of $f_r = 4.5$. Good agreement is obtained for the Reynolds number range of $1 \times 10^6 < R_V < 3 \times 10^6$.

Gertler[31] conducted an extensive set of experiments on various body shapes with the boundary layer tripped at $x = 0.05$. For Gertler's body 4164, the measured[31] and calculated (by the authors) drag coefficients (based on $V^{2/3}$) are 0.0248 and 0.0229, respectively, at $R_L = 10 \times 10^6$. (It was observed that Nash and Hicks' method did not predict C_D very well when the flow over the body was mainly turbulent. The turbulent boundary layer was recalculated by the Head's entrainment method as modified by Shanebrook and Sumner[32] to obtain the improved values of C_D presented in this section.) Hess and Smith[33] obtained $C_D = 0.023$ for the same body using a finite-difference boundary-layer method. For body 4165, the measured[31] and calculated (by the authors) drag coefficients are 0.0188 and 0.0198, respectively, at $R_L = 25.88 \times 10^6$. Parsons and Goodson[34] calculated $C_D = 0.0203$, whereas Zedan and Dalton[35] calculated $C_D = 0.0192$ for the identical body and flow condition.

Optimization Procedure for NLF Body Design

A computational design procedure has been developed to obtain extensive runs of predicted laminar flow over regions of favorable pressure gradient under smooth surface conditions. The method involves a constrained minimization procedure[36] coupled with the aerodynamic analysis program.[21] Initial values of the design variables describing the body shape are input along with length Reynolds number and maximum diameter-to-length ratio. The axisymmetric body is described by seven geometric parameters (k_1, r_i, r_n, s_i, x_i, x_m, ϕ), which are illustrated in Ref. 37.

A number of constraints must be imposed on the design parameters in order to generate designs that are realistic and practical. The necessary geometric constraints follow.

1) $0 < x_m < x_i < 1$
2) $0 \le r_n$
3) $0 \le k_1$
4) $0 \le r_i \le 1$
5) $0 \le s_i$
6) 5 deg $\le \phi \le$ 80 deg
7) No inflection on forebody, midbody, and afterbody, except at x_i.

The aerodynamic constraint is that turbulent separation may not take place before $x = 0.95$. The objective function is C_D in the present investigation and is to be minimized subject to the preceding constraints. The optimizer computes the

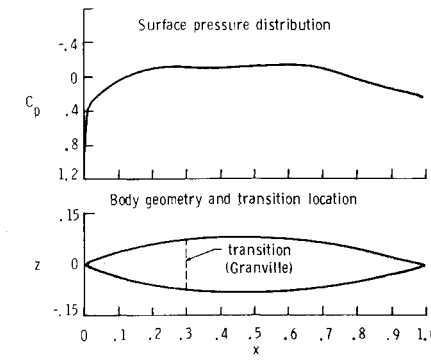

Fig. 10 Pressure distribution, geometry, and transition location for $f_r = 6.14$ body of revolution ($\alpha = 0$ deg, $R_L = 40.86 \times 10^6$).

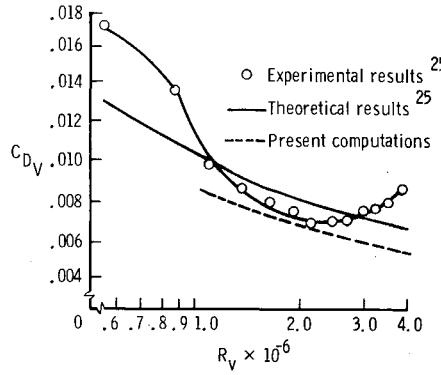

Fig. 11 Comparison of calculated and measured drag coefficients for $f_r = 4.5$ body at $\alpha = 0$ deg.

gradients of the objective function and then, using either a conjugate direction method or a method of feasible direction, determines a linear search direction, along which a new constrained variable is constructed. An improved or minimum feasible objective functional value is evaluated, and a series of proposed updated design variables are calculated. The objective function and the constrained functions are evaluated using the updated design variables and interpolating over the range of feasible proposed design variables resulting in a minimum value of the objective function. The results are then tested against a convergence criterion. The procedure stops if the convergence criterion is satisfied, giving a final design shape with minimum drag satisfying the separation constraint. If the convergence criterion is not satisfied, the design parameters go through the analyzer again, resulting in a new set of design variables, and the procedure is repeated until a final shape is obtained.

Generally, initial application of the optimization procedure results in a minimum drag body shape, which represents a local minimum in the feasible design space. The design parameters obtained are modified slightly and used together with judicious changes in the lower and upper bound of the design variables as new input in the optimization procedure.

Results of the Optimization Study

Some results obtained by the optimization procedure are given in Table 2 for $M = 0$, $\alpha = 0$ deg, $f_r = 6.14$, and $R_L = 40.86 \times 10^6$. First, the axisymmetric body is modeled by a set of initial values of the design parameters. The upper and the lower bounds of the design variables are also input. The design parameters at the end of each iteration are presented in Table 2 along with the objective function and transition location. Since the initial values of the design variables were not too far from the optimized design variables, the design process converged in eight iterations.

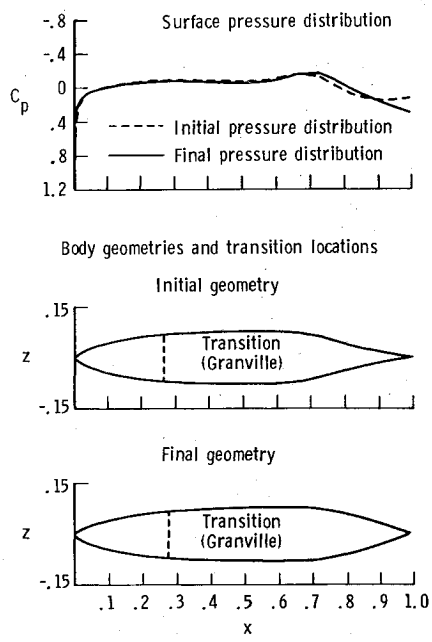

Fig. 12 Characteristics and shapes for initial and optimized body of revolution ($f_r = 6.14$, $R_L = 40.86 \times 10^6$, $\alpha = 0$ deg).

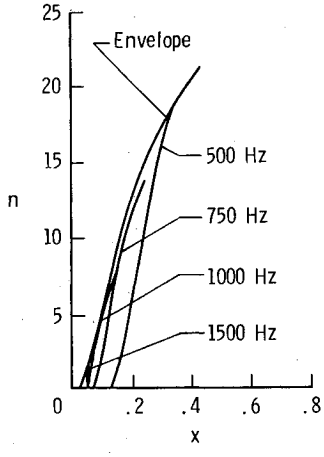

Fig. 13 Incompressible linear stability analysis for optimized body shape at $R_L = 40.86 \times 10^6$ and $\alpha = 0$ deg.

Judicious choice of the starting solution helps in achieving the final optimized solution in a fewer number of iterations. The initial body shape, determined by the design parameters in the first row of Table 2, is shown in Fig. 12. The calculated pressure distribution for the body is also shown in the figure.

For this initial body, transition location was predicted at $x = 0.36$. It is seen from the table, that over several iterations the transition location is pushed further aft and the drag coefficient is reduced. The shape of the final body is also shown in Fig. 12 along with the surface pressure distribution and predicted transition location. Although in this example the movement of the transition point is small, it is seen that the procedure makes it possible to design bodies with long runs of laminar flow starting from a turbulent body. This example also shows that aft-body shape is affected most by selecting C_D as an objective function in the design procedure. Since to date there exists no proven satisfactory method to predict the transitional region on an axisymmetric body of $f_r = 4$–10, Granville's criterion has been used in the optimization cycle. A linear stability analysis was also performed on the optimized body, and the results are shown in Fig. 13. In Fig. 13, n factors are plotted as a function of the nondimensional axial distance x for a range of disturbance

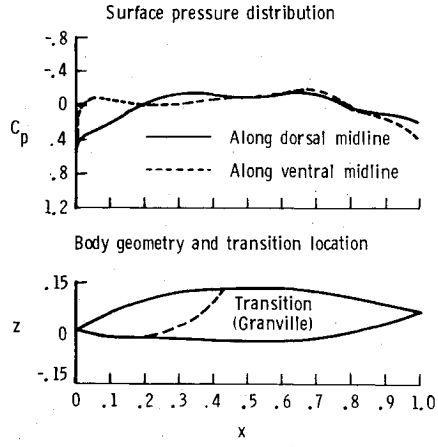

Fig. 14 Characteristics and shapes of fuselage obtained by superimposing camber of body shown in Fig. 9 onto thickness distribution of body shown in Fig. 12 ($R_L = 40.86 \times 10^6$, $\alpha = 0$ deg).

frequencies. From the figure, we see that at $x = 0.24$ an n factor of 15 is reached on this optimized body, which has a fineness ratio of 6.14. In comparison, for the X-35 body, which has a fineness ratio of 4.85, $n = 15$ is reached at $x = 0.3$.

Surface pressure distribution, geometry, and transition location on an improved configuration representative of a business aircraft fuselage are presented in Fig. 14. The fuselage shape was obtained by superimposing the optimized axisymmetric body shape shown in Fig. 12 and the camber distribution of the body shown in Fig. 9. A comparison of the transition location depicted in Fig. 9 (both transition locations are for $R_L = 40.86 \times 10^6$) indicates that use of the optimization method resulted in a longer run of laminar flow than was obtained on the unoptimized shape. Thus, for small modifications in body contours, a significant increase in the extent of laminar flow can be obtained, at least when evaluated using Granville's transition criteria.

Concluding Remarks

Present airplane construction techniques result in the production of smooth and accurate aerodynamic surfaces over which long runs of natural laminar boundary-layer flow (NLF) can be obtained. A major portion of the past research effort for achieving NLF has been focused on airplane lifting surfaces. However, fuselage shaping to achieve considerable regions of NLF has received very limited attention. Recent introduction of business and commuter airplanes with low-drag laminar flow lifting surfaces justifies study of the feasibility of NLF over fuselage surfaces and thereby providing possibilities to decrease airplane profile drag.

A surface singularity analysis method was used to obtain surface pressure distributions over a selected number of body shapes, including a representative nonaxisymmetric business aircraft fuselage. Using an integral boundary-layer method, predictions of transition location and drag coefficient have been obtained for these body shapes. Extensive runs of NLF were predicted over regions of favorable pressure gradient on smooth surfaces of both axisymmetric and nonaxisymmetric bodies at low angles of attack.

The adequacy of existing transition prediction methods applied to bodies was investigated and found to be inadequate to predict transition accurately. This is due partly to the fact that the transition criteria are based on two-dimensional correlations and partly because the criteria validated in the low Reynolds number range are extrapolated beyond the range for which they were validated. The laminar boundary-layer stability theory could be used to make acceptable transition predictions. The state of the art in the prediction of transition is very poor for bodies of fineness ratios between 4 and 10 (of interest for aircraft fuselages) at high length Reynolds

numbers. Much work is needed to account for the stabilizing effects on boundary-layer stability of compressibility and convex curvature, and the destabilizing effects of three-dimensional Tollmien-Schlichting wave stretching and cross-flow vorticity.

It is observed that no high-quality experimental data are available for medium-to-high fineness ratio bodies at representative Reynolds numbers (at least $R_L = 40 \times 10^6$). An experiment should be conducted on a representative body in a large low-turbulence ground facility to obtain surface pressures, boundary-layer velocity profiles, and transition characteristics for a range of angles of attack at high length Reynolds numbers. The results would provide highly necessary data for the validation of computational methods.

A computational design procedure coupled with an aerodynamic analysis program has been developed to obtain low-drag body shapes. Transition location is calculated by using Granville's transition criteria. Results obtained using this procedure show that it is possible to design bodies having relatively high fineness ratios and long runs of natural laminar flow at representative cruise length Reynolds numbers.

Acknowledgment

This research was supported by NASA Langley Research Center under Grant NAG1-345 to University of Kansas and Contract NAS1-17926 to Vigyan Research Associates Inc., Hampton, VA.

References

[1]Runyan, J. L., Navran, B. H., and Rozendal, R. A., "F-111 Natural Laminar Flow Glove Flight Test Data Analysis and Boundary-Layer Stability Analysis," NASA CR-166051, Jan. 1984.

[2]Holmes, B. J., Obara, C. J., and Yip, L. P., "Natural Laminar Flow Experiments on Modern Airplane Surfaces," NASA TP-2256, June 1984.

[3]Quast, A. and Horstmann, K. H., "Profile Design for Wings and Propellers," NASA TM-77785, Nov. 1984.

[4]Williams, K. L., Vijgen, P., and Roskam, J., "Natural Laminar Flow and Regional Aircraft," *SAE Transactions,* Vol. 4, 1985.

[5]Holmes, B. J., Obara, C. J., Martin, G. L., and Domack, C. S., "Manufacturing Tolerances for Natural Laminar Flow Airframe Surfaces," SAE Paper 850863, 1985.

[6]Althaus, D., "Wind-Tunnel Measurements on Bodies and Wing-Body Combinations," *Motorless Flight Research 1972,* NASA CR-2315, Nov. 1973.

[7]Radespiel, R., "Wind Tunnel Investigations of Glider Fuselages with Different Waisting and Wing Arrangements," NASA TM-77014, 1983.

[8]Hertel, H., *Structure-Form-Movement,* Reinhold, New York, 1966.

[9]Carmichael, B. H., "Underwater Drag Reduction Through Optimal Shape," *Underwater Missile Propulsion,* edited by L. Greiner, Compass Publications, Arlington, VA, 1966.

[10]Boltz, F. W., Kenyon, G. C., and Allen, C. Q., "The Boundary-Layer Transition Characteristics of Two Bodies of Revolution, a Flat Plate, and an Unswept Wing in a Low-Turbulence Wind Tunnel," NASA TN D-309, 1960.

[11]Meier, H. U. and Kreplin, H. P., "Experimental Investigations of Boundary-Layer Transition and Separation on a Body of Revolution," *Z. Flugwiss. Weltraumforsch.,* Vol. 4, 1980, pp. 65–71.

[12]Dalton, C. and Zedan, M. F., "Design of Low Drag Axisymmetric Shapes by the Inverse Method," *Journal of Hydronautics,* Vol. 15, Jan.–Dec., 1981, pp. 48–54.

[13]Parsons, J. S., "The Optimum Shaping of Axisymmetric Bodies for Minimum Drag in Incompressible Flow," Ph.D. thesis, Purdue Univ., 1972.

[14]Parsons, J. S., Goodson, R. E., and Goldchmied, F. R., "Shaping of Axisymmetric Bodies for Minimum Drag in Incompressible Flow," *Journal of Hydronautics,* Vol. 8, July 1974, pp. 100–107.

[15]Pinebrook, W. E., "Drag Minimization on a Body of Revolution," Ph.D. thesis, Univ. of Houston, 1982.

[16]Pinebrook, W. E. and Dalton, C., "Drag Minimization on a Body of Revolution Through Evolution," *Computer Methods in Applied Mechanics and Engineering,* Vol. 39, 1983, pp. 179–197.

[17]Wolfe, W. P. and Oberkampf, W. L., "A Design for the Flow Field and Drag of Bodies of Revolution in Incompressible Flow," AIAA Paper 82-1359, 1982.

[18]Barger, R. L., "A Theoretical Investigation of Forebody Shapes Designed for Natural Laminar Boundary-Layer Flow," NASA TP-1375, Jan. 1979.

[19]Hess, J. L., "The Unsuitability of Ellipsoids as Test Cases for Line-Source Methods," *Journal of Aircraft,* Vol. 22, April 1985, pp. 364–367.

[20]Von Kármán, Th., "Calculation of Pressure Distributions on Airship Hulls," NACA TM-574, 1930.

[21]Maskew, B., "Prediction of Subsonic Aerodynamic Characteristics—A Case for Low-Order Panel Methods," *Journal of Aircraft,* Vol. 19, Feb. 1982, pp. 157–163.

[22]Fox, C. H. Jr., "Experimental Surface Pressure Distributions for a Family of Axisymmetric Bodies at Subsonic Speeds," NASA TM X-2439, Dec. 1971.

[23]Groth, E. E., "Boundary-Layer Transition of Bodies of Revolution," Northrop Aircraft Co., Rept. NAI-57-1162, BLC-100, July 1957.

[24]Kaups, K., "Transition Prediction on Bodies of Revolution," Douglas Aircraft Co., Rept. MDC J6530, April 1974.

[25]Hansen, R. J. and Hoyt, J. G., "Laminar-to-Turbulent Transition on a Body of Revolution with an Extended Favorable Pressure Gradient Forebody," *Transactions of the ASME,* Vol. 106, June 1984, pp. 202–210..

[26]Cebeci, T. and Bradshaw, P., *Momentum Transfer in Boundary Layers,* Hemisphere, Washington, 1977.

[27]Wazzan, A. R., Gazley, C. Jr., and Smith, A. M. O., "H-R_x Method for Predicting Transition," *AIAA Journal,* Vol. 19, June 1981, pp. 810–811.

[28]Srokowski, A. J. and Orszag, S. A., "Mass Flow Requirements for LFC Wing Design," AIAA Paper 77-1222, 1977.

[29]Harris, J. E. and Blanchard, D. K., "Computer Program for Solving Laminar, Transitional, or Turbulent Compressible Boundary-Layer Equations for Two-Dimensional and Axisymmetric Flow," NASA TM-83207, Feb. 1982.

[30]Young, A. D., "The Calculation of Total and Skin Friction Drags of Bodies of Revolution at Zero Incidence," ARC R&M 1874, April 1939.

[31]Gertler, M., "Resistance Experiments on a Systematic Series of Streamlined Bodies of Revolution for Application to the Design of High-Speed Submarines," David Taylor Model Basin Rept. C-297, April 1950.

[32]Shanebrook, J. R. and Sumner, W. J., "Entrainment Theory for Axisymmetric, Turbulent, Incompressible Boundary Layers," *Journal of Hydronautics,* Vol. 4, Oct. 1970.

[33]Hess, J. L. and Smith, R. M., "On the Problem of Shaping an Axisymmetric Body to Obtain Low Drag at Large Reynolds Numbers," Douglas Aircraft Co., MDC Rept. J6791, Jan. 1975.

[34]Parsons, J. S. and Goodson, R. E., "The Optimum Shaping of Axisymmetric Bodies for Minimum Drag in Incompressible Flow," Purdue Univ., Rept. ACC-72-6, June 1972.

[35]Zedan, M. F. and Dalton, C., "Viscous Drag Computational for Axisymmetric Bodies at High Reynolds Numbers," *Journal of Hydronautics,* Vol. 13, April 1979, pp. 52–60.

[36]Vanderplaats, G. N., "CONMIN: A Fortran Program for Constrained Function Minimization, User's Manual," NASA TM X-62282, Aug. 1973.

[37]Dodbele, S. S., van Dam, C. P., and Vijgen, P., "Design of Fuselage Shapes for Natural Laminar Flow," NASA CR-3970, March 1986.